Planta
DOI 10.1007/s00425-006-0363-4

ORIGINAL ARTICLE

A cortical band of gelatinous fibers causes the coiling of redvine tendrils: a model based upon cytochemical and immunocytochemical studies

Christopher G. Meloche · J. Paul Knox · Kevin C. Vaughn

Received: 2 June 2006 / Accepted: 18 July 2006
© Springer-Verlag 2006

Abstract A cortical band of fiber cells originate de novo in tendrils of redvine [*Brunnichia ovata* (Walt.) Shiners] when these convert from straight, supple young filaments to stiffened coiled structures in response to touch stimulation. We have analyzed the cell walls of these fibers by in situ localization techniques to determine their composition and possible role(s) in the coiling process. The fiber cell wall consists of a primary cell wall and two lignified secondary wall layers (S_1 and S_2) and a less lignified gelatinous (G) layer proximal to the plasmalemma. Compositionally, the fibers are sharply distinct from surrounding parenchyma as determined by antibody and affinity probes. The fiber cell walls are highly enriched in cellulose, callose and xylan but contain no homogalacturonan, either esterified or de-esterified. Rhamnogalacturonan-I (RG-I) epitopes are not detected in the S layers, although they are in both the gelatinous layer and primary wall, indicating a further restriction of RG-I in the fiber cells. Lignin is concentrated in the secondary wall layers of the fiber and the compound middle lamellae/primary cell wall but is absent from the gelatinous layer. Our observations indicate that these fibers play a central role in tendril function, not only in stabilizing its final shape after coiling but also generating the tensile strength responsible for the coiling. This theory is further substantiated by the absence of gelatinous layers in the fibers of the rare tendrils that fail to coil. These data indicate that gelatinous-type fibers are responsible for the coiling of redvine tendrils and a number of other tendrils and vines.

Keywords Cellulose · Coiling · Fiber cells · Immunocytochemistry · Lignin · Xylan · Control of coiling · Pectin

Abbreviations

S	Secondary
G	Gelatinous
TEM	Transmission electron microscopy
CMF	Cellulose microfibril
RG-I	Rhamnogalacturonan-I
HG	Homogalacturonan
PGA	Polygalacturonic acid

Introduction

The coiling of tendrils has long fascinated botanists and Darwin devoted a whole monograph to the coiling and twining behavior of vines and tendrils (Darwin 1875). When a tendril touches an object, it rapidly wraps around the object, securely attaching to it as a support and guying the vine close to the object (Jaffe and Galston 1969). In this process, the tendril goes from a supple straight organ to one that is relatively rigid and coiled. How the vine senses the touch and how the tendril moves to coil around the support remain active areas of research in plant biology. The most comprehensive physiological studies center on the leaflet tendrils of pea (reviewed by Jaffe and Galston 1969; Jaffe

C. G. Meloche · K. C. Vaughn (✉)
Southern Weed Science Research Unit, USDA-ARS,
P.O. Box350, Stoneville, MS 38776, USA
e-mail: kvaughn@ars.usda.gov

J. P. Knox
Centre for Plant Science, University of Leeds,
LS2 9JT Leeds, UK

1980) and conclude that tendrils are touch-sensitive organs that respond to the touch by elongating on the side away from the touch and contracting on the side nearest the touch. This asymmetric growth pattern results in a net coiling of the organ around the touched surface. Pea is a leaflet tendril, however, and its growth pattern might not be typical of those tendrils that are shoot or whole-leaf tendrils. Moreover, from our studies (C.G. Meloche and K.C. Vaughn, submitted), we suggest that the differential elongation theory for the winding behavior of tendrils does not explain all cases of how tendrils develop or function at maturity.

In a companion study (C.G. Meloche and K.C. Vaughn, submitted), we have observed that the tendril leaves of redvine [*Brunnichia ovata* (Walt.) Shiners] attain their maximal length before they begin to coil. A band of unique, presumably gelatinous, fiber cells appears de novo as the tendril converts from straight to highly coiled, actually shortening and thickening the tendril. Gelatinous-type fibers are widespread in the xylem of angiosperms, notably in reaction wood (White and Robards 1965; Fisher and Tomlinson 2002), but as far as we are aware there is no previous report of extraxylary gelatinous fibers, although other fibers are common constituents of non-woody stems (Esau 1977; Zhong et al. 2001; Goujon et al. 2003). We have proposed that these fiber cells may be a causative agent in allowing the tendril to coil and also rigidifying the tendril into its final position, acting like the gelatinous fibers in righting branches of trees (White and Robards 1965; Yoshizawa et al. 2000).

In this study, we report the distribution of the major constituents of the presumptive gelatinous fiber cell walls of redvine tendrils. The composition and organization of these cells is unique from anything we have observed in herbaceous plants.

Materials and methods

Plant material

Plants of redvine [*B. ovata* (Walt.) Shiners] were grown either from seed or from rhizome pieces in a 1:1 mixture of native Dundee loam and a potting mix consisting of ground pine bark, peat and perlite (2:2:1). Leaf tendrils of redvine were collected both in the elongated but not coiled state and after coiling had commenced. In some cases, tendrils were tracked from their inception and fixed at 3, 4 and 5 days from inception, which represent the states prior to and during potential coiling. Another group of tendrils that had elongated but failed to coil even after 2 months, were also examined. In all cases described herein, the organ sampled is a tendril leaf, although there is also a portion of the tendril that is a stem as well.

Microscopy

For standard electron microscopy, small tendril segments were cut in drops of 6% (v/v) glutaraldehyde in PIPES buffer (pH 7.4) and transferred to scintillation vials containing the same solution for 2 h at room temperature. After two, 15 min washes with 0.1 M sodium cacodylate (pH 7.2), the samples were post-fixed in 2% (w/v) osmium tetroxide in cacodylate buffer for an additional 2 h. After two water rinses, the samples were stained en bloc with 2% uranyl acetate for 18 h at 4°C. The samples were then washed with water, dehydrated in acetone and transferred into propylene oxide. Embedding was carried out by adding 25% (v/v) increments of a 1:1 mixture of Spurr's and epon resins and using half of the catalyst used in the standard Spurr's plastic recipe in 2 h increments up to 75% (v/v) plastic. The remaining 25% (v/v) propylene oxide was allowed to evaporate slowly by placing aluminum foil lids with small holes on top of the vials, so that the increase to 100% resin occurred slowly overnight. New resin was added to these samples and the tubes were shaken on a rocker for 24 h prior to polymerization. Specimens were flat-embedded in BEEM flat embedding molds for 24 h at 58°C in a vacuum oven. Before sectioning, the samples were cut from the blocks with a jeweler's saw and mounted on acrylic stubs to obtain tendrils with cross and longitudinal orientations as needed. Blocks were cut with a Reichert Ultracut ultramicrotome at ~100 nm and mounted on 300-mesh copper grids. Specimens were observed at 60 kV using a Zeiss EM 10CR electron microscope.

Immunocytochemistry

For light microscopic immunocytochemistry, samples were fixed in 3% (v/v) glutaraldehyde in 0.05 M PIPES buffer (pH 7.4) for 2 h at room temperature. After two, 4°C PIPES buffer washes, the samples were dehydrated through ethanol at 4°C and transferred to −20°C. Samples were embedded in LR White resin, by increasing the increments of plastic by 25% each day, with two final exchanges of 100% resin. The vials were then returned to room temperature and shaken on a rocker for 24 h. Samples were cured in BEEM capsules in a vacuum oven. At 50°C, polymerization took place in ~2–4 h under these conditions.

Samples were sectioned at 0.35 μm and dried down to slides coated with chrome-alum on a warming tray.

Sections were placed inside a circle made by a wax pencil that formed a well for the subsequent solutions. Slides were then processed as follows: 1% (w/v) bovine serum albumin (BSA) in phosphate-buffered saline (PBS), 30 min; primary antibody (neat to 1:80), 4 h; four exchanges of PBS–BSA, 10 min total; secondary antibody-colloidal-gold (15 nm, prepared by EY Laboratories), 30 min; three rinses with distilled water; Amersham InstenSE silver intensification kit for microscopy, 15–30 min. The sections were then washed in water, dried and mounted in Permount. Sections were photographed with a Zeiss Axiophot microscope.

For TEM immunocytochemistry, two protocols were followed. One used sections from epoxy resin blocks prepared as described for electron microscopy (above) but the material was mounted on 300-mesh gold grids rather than copper. The other protocol used the same processing steps as described for light immunocytochemistry except that the samples were cut at 100 nm and mounted on 300-mesh gold grids rather than on slides. For both sorts of processing, the samples were handled as described above for light immunocytochemistry except that the samples were floated on 4 µl drops of solutions and no silver intensification step was utilized. Prior to examination, the samples were post-stained with 2% uranyl acetate (2 min) and Reynold's lead citrate (30 s). Immunogold label was counted manually and the density of gold label determined as described previously (Sabba et al. 1999; Vaughn 2006) and expressed as gold particles/µm^2 of wall. Some grids were treated prior to immunogold processing, by floating on drops of 0.5 M sodium carbonate for 1 h prior to immunogold labeling to de-esterify esterified PGAs. These sections were washed with water and then processed as for other immunogold samples.

Cytochemical stains

Lignin stains

Lignin was visualized by its reaction with potassium permanganate, either as an en bloc treatment prior to embedding or as post stain on the embedded material.

Pre-embedding lignin stain

Samples were stained in 1% potassium permanganate for 1 h at room temperature (Hepler et al. 1970; Donaldson 2001). The samples were washed extensively so that the rinsates were free of purple stain and then the samples were processed as described above for standard electron microscope processing (above) except that the samples were not post-stained prior to examination.

Post-embedding lignin stain

Samples prepared for electron microcopy were cut and placed on 300-mesh gold grids and the grids floated on drops of 1% potassium permanganate in 0.1% sodium citrate for 5–7 min (He et al. 2002). Samples were examined without further staining.

Cellulose-binding probe

Material embedded as described for light microscopic immunocytochemistry (above) was sectioned at ~100 nm and mounted on gold grids. The samples were then incubated on drops of the following solutions and times, modified from the McCartney et al. (2004) protocol: 1% (w/v) BSA in PBS, 30 min; 1 µg/ml polyhistidine-tagged CBM3a cellulose-binding carbohydrate-binding module (CBM) in PBS/BSA, 4 h; PBS/BSA, 4 drops, 10 min total; mouse anti poly-his monoclonal (Sigma), diluted 1:80 in PBS/BSA, 1 h; 4 drops, PBS/BSA, 10 min total; goat anti-mouse IgG and M labeled with 15 nm gold (EY Labs), diluted 1:20 in PBS/BSA, 1 h; 4 drops PBS, over 10 min. The grids were then washed in water, dried and then post-stained with uranyl acetate (2 min) and Reynold's lead citrate (30 s) before observation.

Antibodies and controls

Many of the antibodies used in this study are ones that have been used previously by us and are well characterized (e.g., Vaughn et al. 1996; Sabba et al. 1999; Vaughn 2003, 2006; Ligrone et al. 2002). Of the antibodies not previously reported from this laboratory, the two anti-xylan monoclonal antibodies, LM10 and LM11, bind to low substituted xylan and LM11 binds in addition to arabinoxylan (McCartney et al. 2005). Control experiments consisted of no primary antibody or primary antibody or probe that has been reacted with an appropriate substrate (e.g., pachyman for the callose antibodies). All of these control experiments gave label densities >0.3 gold particles/µm^2. For details and references for all probes used see Table 1.

Results

Composition and organization of the polysaccharides within the fibers: light immunogold-silver analysis

We analyzed the composition of the fiber cells from coiled tendril segments by probing semi-thin sections of LR White-embedded material with antibodies to

Table 1 Antibodies and probes used for characterization of fiber cell walls

Antibody/probe	Antigens/epitopes	Reference/source
Xyloglucans		
CCRCM1	Fucosylated xyloglucans	Freshour et al. (1996)
Xyloglucan polyclonal	Xyloglucans	Moore et al. (1986)
Pectins		
JIM5	HG	Clausen et al. (2003)
JIM7	HG	Clausen et al. (2003)
CCRCM2	RG-I	Puhlman et al. (1994)
LM5	1→4-galactan/RG-I	Jones et al. (1997)
LM6	1→5-arabinan/RG-I	Willats et al. (1998)
PGA polyclonal	De-esterified HG	Moore et al. (1986)
Callose		
Callose monoclonal	Callose (pachyman)	Meikle et al. (1991)
Callose polyclonal	Callose (pachyman)	Northcote et al. (1989)
Extensins		
LM1	Extensin	Smallwood et al. (1995)
JIM11	Extensin	Smallwood et al. (1994)
JIM12	Extensin	Smallwood et al. (1994)
Xylans		
LM10	Xylan	McCartney et al. (2005)
LM11	Xylan/arabinoxylan	McCartney et al. (2005)
AGPs		
AGP monoclonal	AGPs	Anderson et al. (1984)
CCRCM-7	AGP, RG-I	Puhlman et al. (1994)
LM2	AGP	Smallwood et al. (1994)
Cellulose		
CBM3a	Cellulose-binding probe	McCartney et al. (2004)

cell wall components (Fig. 1; Table 1) and visualized these reactions with immunogold and subsequent silver intensification. The strong black silver depositions present at the sites of immunological reactivity give an unequivocal localization of each of these components and provide a semi-quantitative estimation of their distribution (Table 2).

Sections stained with Toluidine blue show the arrangement of epidermis, cortical parenchyma and fibers in the tendril cross-section (Fig. 1a). A serial section labeled with the JIM5 a monoclonal antibody that recognizes primarily de-esterified homogalacturonan (HG) monoclonal shows a much different pattern however, with the fiber layer being relatively unlabeled compared to the epidermis and cortical tissue (Fig. 1b). JIM5 reaction is restricted to the middle lamellae in the band of fiber cells. Other antibodies to HG (JIM7 and a PGA polyclonal antibody) react with either the middle lamella (PGA) or weakly with the primary walls but not elsewhere in the fiber cells (JIM7), leaving the secondary walls of the fibers in negative relief (not shown; Table 2). LM5 and LM6 recognize the (1→4)-galactan and (1→5)-arabinan side groups of rhamnogalacturonan-I (RG-I), respectively, and these antibodies did not label the S_1 or S_2 layers of the fiber, but did label the presumed gelatinous layer and material that was probably part of the primary wall at the middle lamellae interface (Fig. 1d, e). The labeling with these antibodies between adjacent fiber cells was more intense than the labeling between cells in other tissues of the redvine tendril. CCRCM2 that also recognizes a RG-I epitope showed a similar distribution of label (Table 2). In contrast to the labeling pattern of the HG and RG-I antibodies, antibodies to xyloglucans labeled both fiber and non-fiber cells (e.g., Fig. 1c).

Callose antibodies also label the fiber cells, although the pattern of label on these cells is more diffuse than noted with the anti-xyloglucan (not shown). A similar sort of diffuse localization was noted using any of three different extensin monoclonal antibodies, alone or together. However, both the callose and extensin antibodies labeled the fiber cells, much more so (callose) or exclusively (extensin) than the surrounding parenchyma cells (Table 2). Antibodies to glycan components of arabinogalactan-proteins (Australian monoclonal, LM2, JIM8 and CCRCM7) did react with the fiber cells, but generally only at the plasma membrane or occasionally with the middle lamella/wall interface (not shown).

The strongest labeling specific to the fiber cells occurred with two anti-xylan antibodies LM10 and LM11. Both of these antibodies strongly reacted with

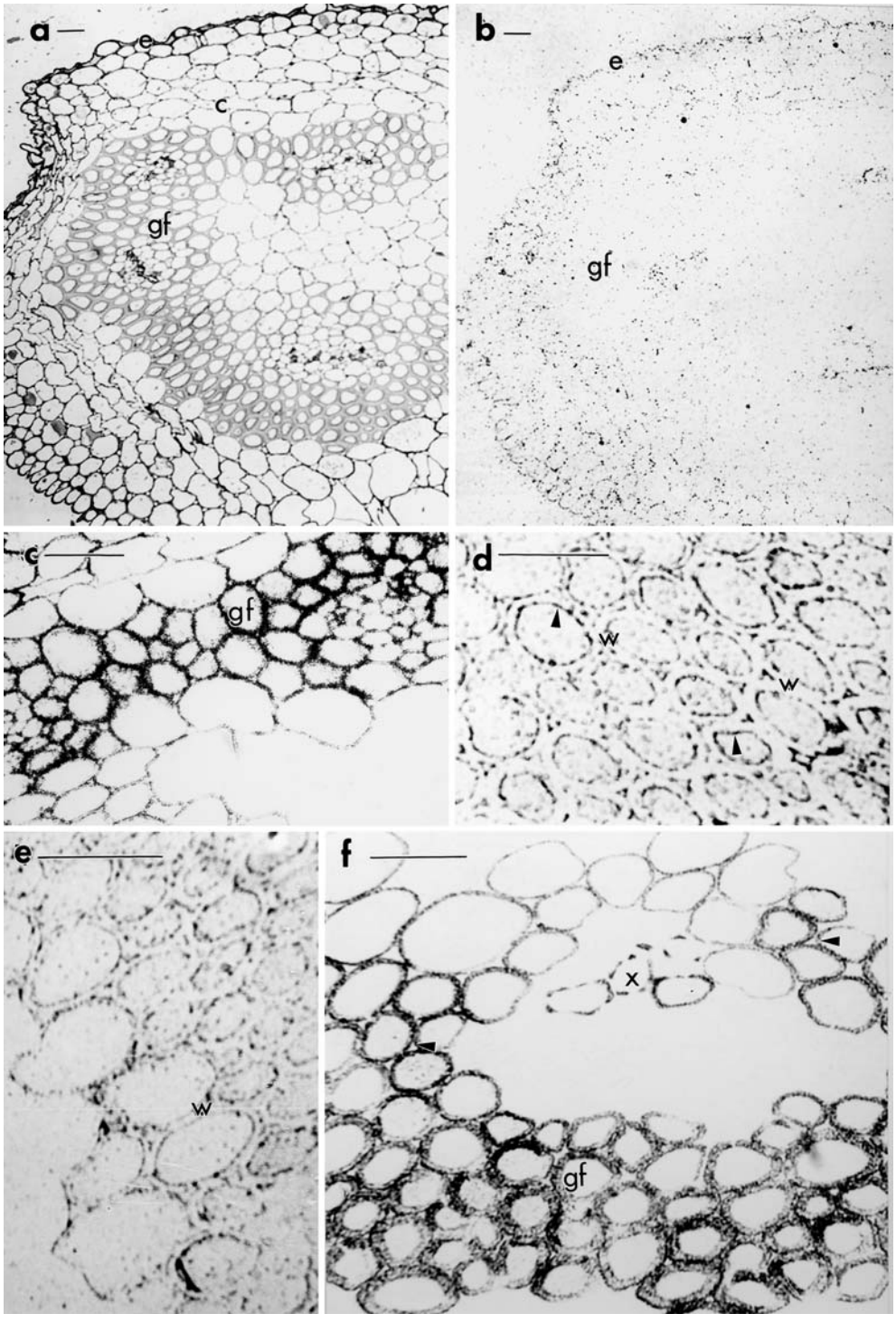

Fig. 1 Light microscopy (*A*) and immunogold-silver (*B–F*) of coiled redvine tendrils. **a** Light microscopic section serial to that used for the immunogold-silver analysis. Note the thick band of fiber cells (*gf*) adjacent to the cortical cells (*c*). **b** Section immunolabeled with JIM5 (highly de-esterified pectin) reveals no label on the fiber cells (*gf*) per se (weak label on middle lamellae) but strong label on cortical and epidermal cells (*e*). **c** Region of fiber cells (*gf*) and adjacent cortical cells labeled with anti-fucosylated xyloglucan antibodies. Note strong label on fiber cells (*f*). **d** and **e** Label with LM5 (**d**) and LM6 (**e**) that label side chains on RG-I reveal a similar pattern of labeling. The secondary layers of wall (*w*) in the fiber cells are not labeled but the inner layer of the fiber (*arrowheads* in **d**) and a small layer near cell corners and along the primary wall are strongly labeled. **f** Strong label on fiber cells (*gf*) and xylem elements (*x*) with the LM11 antibody that recognizes xylans. *Bars* = 100 μm

Table 2 Light microscopic immunogold-silver localization of polysaccharide and glycoproteins in fibers and other cells of red-vine tendrils

Antibody	Fiber	Parenchyma	Other
Xyloglucans			
CCRCM-1	++	+	Vascular
Xyloglucan poly	++	+	Vascular
Pectins			
JIM5	−	+	ML[a]
JIM7	−	+	
CCRCM2	−	+	
LM5	±[b]	+	
LM6	±[b]	+	
Pectin polyclonal	−	+	ML[a]
Callose			
Monoclonal	+	−	PD[c]
Polyclonal	+	−	PD[c]
Extensin			
LM1	+	−	
JIM11	+	−	
JIM20	+	−	
Xylan			
LM10	++	−	Xylem
LM11	++	−	Xylem
AGPs			
CCRCM7	+	+	
LM2	+	+	
Monoclonal	+	+	

++ indicates strong reaction, + indicates average reaction, − indicates no reaction

[a] Middle lamellae

[b] Only in gelatinous layer and pre-existing primary wall. Strong reaction between cells

[c] Plasmodesmata

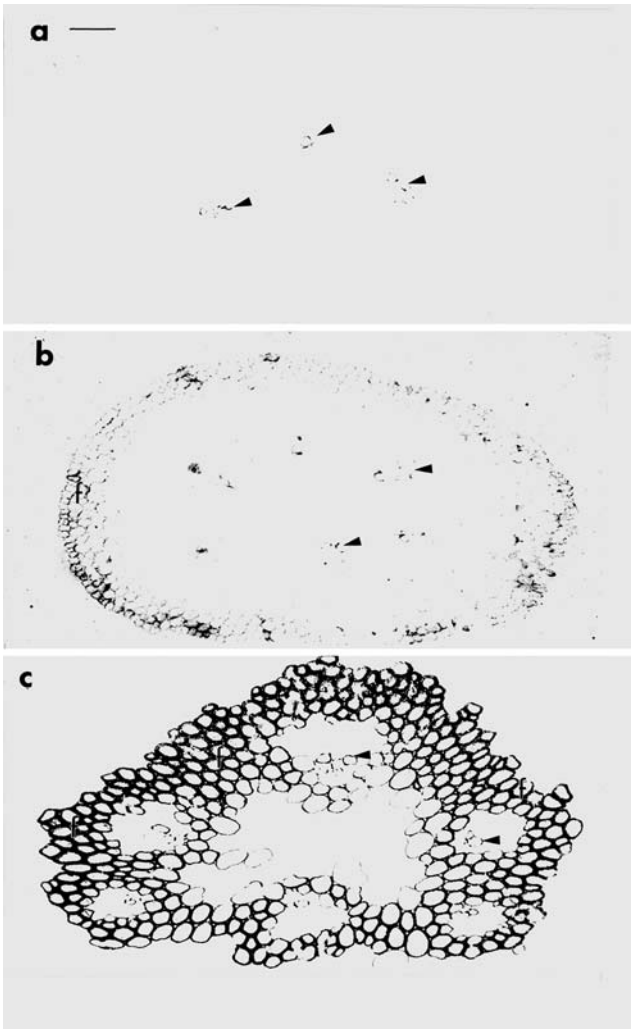

Fig. 2 Labeling of day 3 uncoiled (**a**), day 4 uncoiled (**b**) and day 5 coiled (**c**) tendrils with the LM10 antibody. In day 3 tendrils that are not coiled, the only labeling observed is associated with the secondary walls of xylem elements (*arrowheads*). In the 4-day-old tendrils, the band of fibers (*f*) is beginning to be formed and is labeled lightly with the LM10 antibody as well as the xylem elements (*arrowheads*). In 5-day-old tendrils, the label is strong throughout the band of fiber cells (*gf*). The xylem elements (*two marked with arrowheads*) are also labeled. Bar = 100 μm

the fiber cells and the secondary walls in xylem elements (Figs. 1f, 2). These antibodies provided a reliable and strong marker for the appearance of these fibers. Three-day-old tendrils, prior to any coiling, reacted only in the xylem elements (Fig. 2a). When tendrils were examined in the process of coiling, fibers were formed and LM10 and LM11 epitopes were present as soon as indications of secondary wall formation in the fiber cells were noted. Four days after emergence of the tendril, the fibers have just begun to form. These appear to be forming at the edge of the cortical band of tissue and progress inward toward the vascular tissue (Fig. 2b). By day 5, the fiber cells had fully formed and were strongly labeled with either the LM10 or LM11 antibodies (Fig. 2c).

In addition to the differences in LM10 and LM11 labeling of the immature fibers, there were also differences in the distribution of LM5, LM6 and callose epitopes (not shown). In the 4-day-old tendrils, LM5 and LM6 epitopes were found throughout the parenchyma cell walls whereas in the fiber cells these epitopes were only observed in old primary wall/middle lamellae interface, indicating that the G layer had not yet formed. Although callose was detected in mature fibers, it was not observed at the light level in the 4- or 5-day-old fiber cells.

Although the composition of fiber cell walls was atypical, the labeling pattern of the parenchyma and vascular tissues in the tendril were much as expected for primary dicotyledonous plant cell walls (Table 2), indicating that in the twining tendril, the fibers are the previously undocumented cell type.

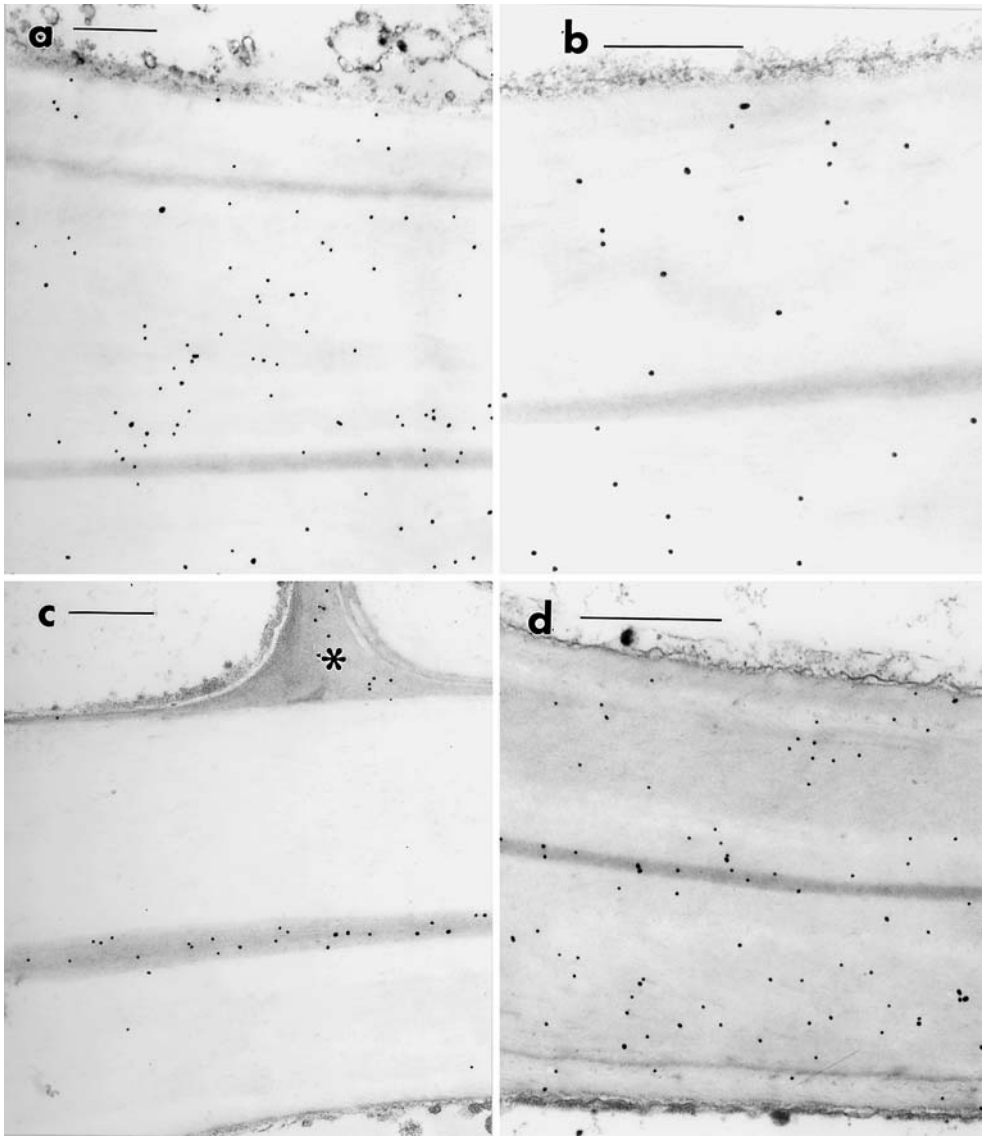

Fig. 3 Immuno- and affinity-localizations of polysaccharides in fiber cells. **a** Polyclonal anti-xyloglucan labels all of the fiber layers. **b** Monoclonal anti-callose labels S layers but not compound middle lamellae/primary wall nor the G layer. **c** Polyclonal anti-PGA after sodium carbonate treatment reveals staining only in the middle lamellae/primary wall complex and the primary walls of adjacent parenchyma cells (*asterisk*). **d** Cellulose-binding probe labels all of the layers of the fiber. *Bars* = 0.5 μm

Immunogold TEM localization

Using TEM immunogold, we determined the patterns of cell wall labeling indicated by the light immunogold-silver localizations (above) in more detail. In some antibody localizations, we were able to use sections that had been prepared for traditional electron microscopy, whereas for other antibodies, un-osmicated tissues embedded in LR White resin were used.

The xyloglucan polyclonal (Fig. 3a) and the CCRCM-1 antibodies (not shown) labeled all of the layers in the fiber, including the compressed primary wall and middle lamellae, with a relatively even distribution. Although in fiber cells, xyloglucans are generally replaced by xylans, these cells are strongly labeled with two different antibodies. Perhaps the rapid synthesis of secondary walls has made these cell walls more flexible in the use of other polysaccharides in secondary cell wall assembly.

Callose antibodies gave a diffuse localization over the fiber cells using immunogold-silver (discussion above) and on the TEM level this same sort of diffuse and uneven reaction was noted. Callose occurred throughout the fiber cells, sometimes in clumps in less electron opaque areas of the wall, although the amount of label in the gelatinous layer was much less than in

Table 3 Quantification of immunogold and affinity-gold labeling in fiber cells of red-vine tendrils

Antibodies	Labeling density (gold particles/μm^2) ± SE
Xyloglucans	
CCRCM-1	97 ± 6
Xyloglucan polyclonal	114 ± 8
Pectins	
JIM5[a]	0.2 ± 0.2
JIM7[a]	3 ± 1
CCRCM-2[b]	18 ± 4
LM5[b]	39 ± 4
LM6[b]	27 ± 4
Pectin polyclonal[a]	2 ± 1
Callose	
Monoclonal[c]	47 ± 17
Polyclonal[c]	51 ± 22
Extensin	
LM1[c]	11 ± 3
Xylans	
LM10	209 ± 39
LM11	72 ± 17
Cellulose	
CBM3a cellulose-binding probe	127 ± 22

Data are from 18 or more micrographs. Collection and processing of data were as described by Sabba et al. (1999) and Vaughn (2006)

[a] Does not include reaction in middle lamellae

[b] Reaction specific to the gelatinous layer

[c] Reaction found only in the S_1 and S_2 layers

the S_1 or S_2. A mid-range level of labeling is noted in the fiber cell shown in Fig. 3b. Because both polyclonal and monoclonal antibodies exhibited these reactions, we can eliminate possibilities of artifactual localizations. The amount of label on any given fiber cell varied tremendously from fiber to fiber, with values as low as 7 gold particles/μm^2 up to 72 gold particles/μm^2, even when fiber cells in the same hole on the TEM grids are compared (Table 3). Plasmodesmal collars of both the fiber cells and the surrounding parenchyma cells were strongly labeled as well, although other areas of the wall were not in the parenchyma cells. Moreover, pre-incubation of the callose monoclonal or polyclonal antibodies with pachyman (a 1→3-glycan that was used in the initial antigen in eliciting antibodies) resulted in no subsequent section labeling.

The cellulose probe labeled throughout the layers of the fiber and at relatively high levels of labeling (Fig. 3d; Table 3). Some label was observed at the middle lamella/primary wall, presumably due to reactions with old primary wall and/or non-specific reactions with pectins. The cellulose-binding probe showed more background reactions (~3–4 gold particles/μm^2 on acellular areas of the plastic) than the antibody probes on non-cellular structures but was superior to cellulase-gold probes previously used in our laboratory (e.g., Sabba et al. 1999).

Analysis of HGs confirmed and extended observations made at the light microscopic level. JIM5 and the PGA polyclonal antibody epitopes were confined to the middle lamella and, even after the sections had been treated overnight in sodium carbonate to de-esterify all the residues, no reaction was noted over any of the fiber cell secondary wall layers (Fig. 3c). Adjacent parenchyma cells did react both in the primary wall (after de-esterification) and in the middle lamella (either untreated or after de-esterification), however. Similarly, labeling with JIM7 that can recognizes more highly esterified HG, did not label fiber cells, with the exception of some weak binding at the middle lamellae/primary wall (not shown).

Both LM5 (Fig. 4a) and LM6 (Fig. 4b) antibodies strongly labeled an inner cell wall band in the light sections and we observe this same labeling pattern at the TEM level. Although detachment of the gelatinous layers is considered an artifact of preparation (Clair et al. 2005), we did observe that, toward the cut ends of samples, detached gelatinous layers that were well labeled with the LM5 or LM6 antibodies (not shown) as a further indication that only the gelatinous layer was labeled. In addition to the label in the gelatinous layer, both LM5 and LM6 antibodies labeled a zone of cell wall adjacent to but not including the middle lamella (Fig. 6a), which probably represents an area of the primary wall that is generally unresolved in the compound middle lamellae/primary wall complex by standard post-staining protocols.

As might be expected, anti-xylan LM10 (Fig. 6c) and LM11 (not shown) gave a very strong labeling of the fiber cells and xylem elements and the labeling was clearly restricted to those cells or an occasional neighboring cell that had begun to thicken. Labeling with

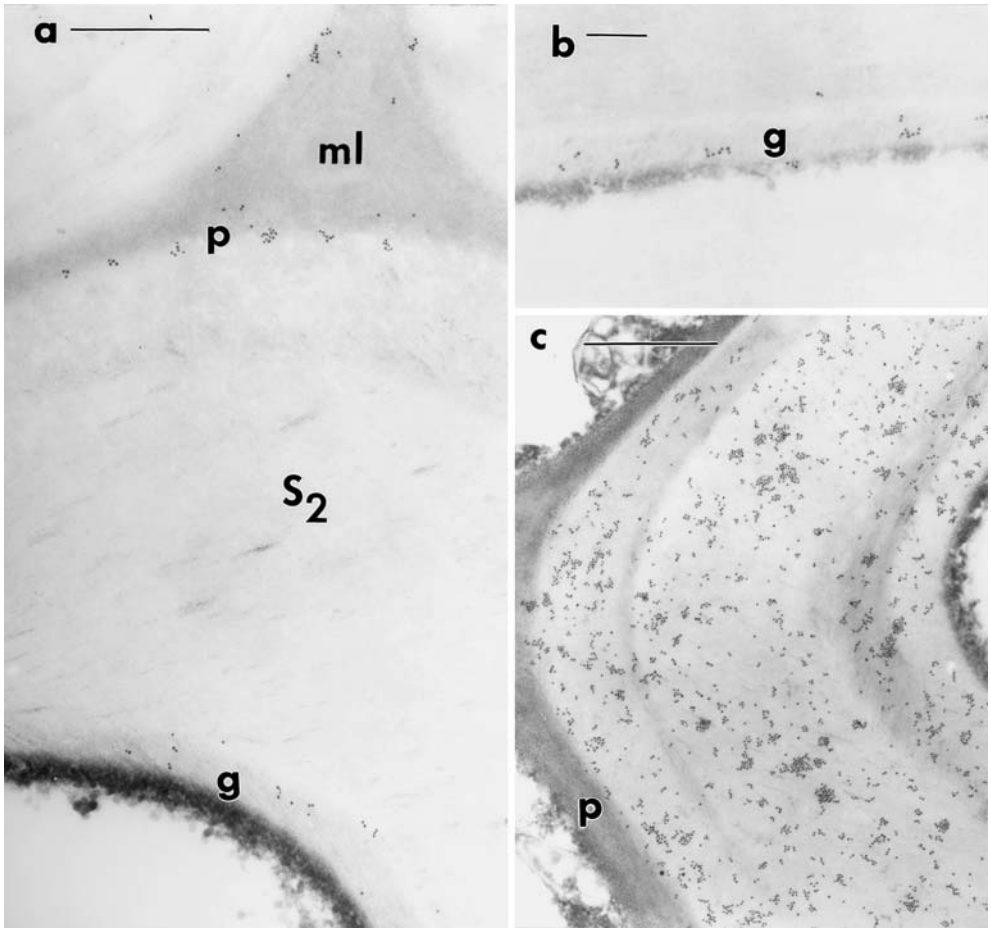

Fig. 4 Immunogold localizations in fiber cells. **a** Anti-galactan side chain antibody LM5 reacts with the gelatinous (*g*) layer and a layer of wall, presumably primary wall (*p*) that borders the middle lamellae (*ml*). **b** The gelatinous layer (*g*) is strongly labeled with anti-arabinan side chain antibody LM6. **c** Anti-xylan LM10 labeling is intense throughout the fiber cell but does not label primary walls of adjacent parenchyma or its own primary wall. *Bars* = 0.5 μm in (**a** and **c**), 0.2 μm in (**b**)

LM10 was more uniform across the tissue than LM11, which appeared in intense pockets throughout the fibers. Because LM10 labels more highly substituted xylans, this might indicate a unique organization of the xylans in the gelatinous fibers. A similar level of labeling was noted on xylem elements found in these same sections, although the LM11 was more uniform (not shown).

Probing of uncoiled 4-day-old tendrils reveal the appearance of LM10 and LM11 epitopes in the newly formed S_1 layer, although at much lower levels than in the more mature fibers or in adjacent xylem elements (not shown). LM5 and LM6 epitopes were restricted to the middle lamella/primary wall interface, indicating that the G layer had not formed at this time, prior to any coiling. Callose, although widespread at later stages in the S_1 and S_2 layers in mature fibers, was present only in plasmodesmata collars in the immature fibers (not shown).

Quantification of immunogold labeling at the TEM level confirms the qualitative evaluation at the light microscopic level as well (Table 3). Only data for fibers is included here. Although callose labeling was highly variable (Table 3), results with the other antibodies and probes was quite consistent, generally with a standard error of less than 10%.

Lignin cytochemistry

Lignin, as revealed by pre- or post-embedding permanganate stains, was not found in every fiber cell, especially in those tendrils where coiling had just commenced, indicating that lignification is one of the latter steps in the differentiation of the cortical fiber cells (Fig. 5a). Lignin staining appeared to be more consistent and strongest on the side nearest the touched surface on the coiled tendril. Within the fiber cell, strong reaction is noted in the middle lamella/

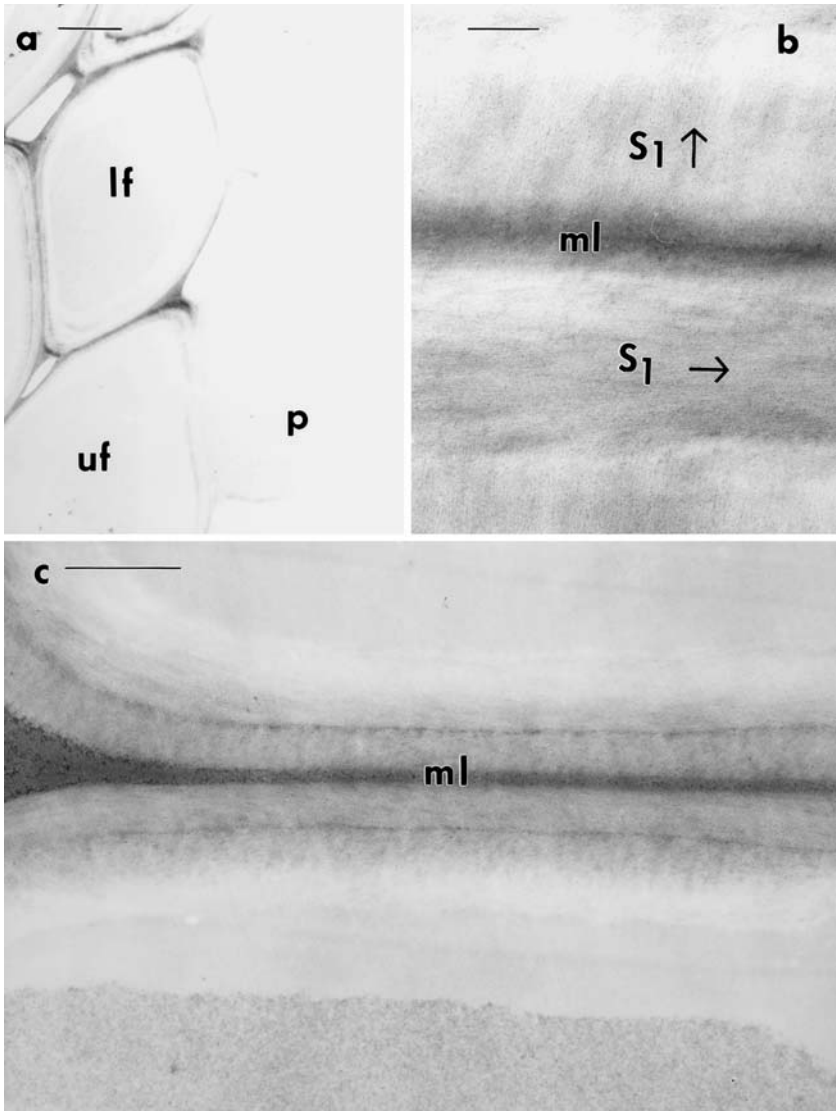

Fig. 5 Permanganate staining for lignin. **a** A low magnification micrograph through a tendril that is early in the coiling process containing both lignified (*lf*) and un-lignified (*uf*) fiber cells. No reaction is noted in parenchymatous (*p*) cells. **b** Apparent alternation of cellulose microfibril orientation in adjacent fiber cells. In these two cells the lignin staining reveals that the CMF in the S_1 layers of the two cells are oriented perpendicular to each other (*arrows* indicate direction of CMF orientation). **c** Two adjacent cells fiber stained for lignin reveals strong staining of the primary wall/middle lamellae complex (*ml*) and the S_1 layer but weaker staining in the S_2 and almost none toward the periphery of the cell, including the gelatinous layer. *Bars* = 1.0 μm in (**a**), 0.2 μm in (**b**) and 0.5 μm in (**c**)

primary wall and in the S layers of the fiber, with relatively little in the gelatinous layer. Interestingly, the lignin staining protocols allow for a good visualization of the orientation of cellulose microfibrils as they stand out in negative relief (Fig. 5b). Adjacent fiber cells in twisted tendrils appear to have cellulose microfibrils in different orientations, often perpendicular to each other (Fig. 5b). Strong reactions for lignin in the middle lamellae/primary wall and S layers and a lack of reaction in the G layer are also noted in gelatinous fibers of many other species (Donaldson 2001).

When nascent uncoiled fibers (from tendrils 4 days after emergence) are monitored with the lignin stains, the S_1 layer is the only one present, but in these sections the orientation of the cellulose microfibrils appears to be identical in all fiber cells. Thus, the apparent random orientation of the cellulose microfibrils observed in coiled tendrils is probably the result of the twisting of the segments. This could occur because of the true twisting of the cells (or even layers within the wall) or the variety of orientations of the cells in a cross-section cut across a highly coiled structure.

Tendrils that fail to coil

Generally redvine tendrils follow two modes of coiling (C.G. Meloche and K.C. Vaughn, submitted). Tendrils that have been touch-stimulated coil about the touched object, guying the stem close to the support. Tendrils that fail to touch an object, form what is termed a free coil, with the tendril coiled along half its length in one direction and half its length in the other. Although most redvine tendrils do one of these two functions, a minority (~1%) of tendrils remain uncoiled even as long as 2 months after appearance (unpublished; C.G. Meloche

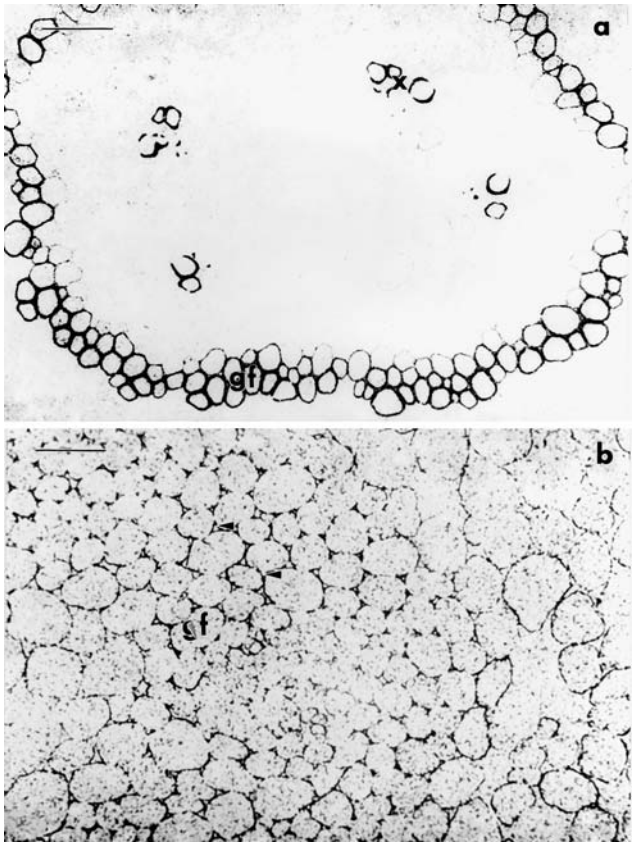

Fig. 6 Immunocytochemistry of tendrils that failed to coil. **a** After LM10 labeling of sections, a layer of fibers is revealed and strong xylem labeling is noted. **b** Labeling with LM6 antibodies to an arabinan side chain of RG-I reveals labeling of the primary walls of all cells and additional labeling around the cell–cell junctions in between adjacent fiber cells. However, unlike fibers in tendrils that coil (Fig. 1d, e), there is no internal layer of labeling in these cells, even after over-exposure of the sections to primary antibody. *Bars* = 100 μm

and K.C. Vaughn, submitted). When these tendrils are monitored by light microscopy, a layer of fibers is present, but it is much less developed than in coiled tendrils (not shown). Generally only 1–2 cell layers of fibers cells are formed compared to the 5–6 layers in coiled tendrils. In many ways, these are similar to the immature, 4-day-old tendrils described above.

Compositionally these fiber cells are also distinct from those in the coiled tendrils. The fibers do react strongly with antibodies to the xylans LM10 and LM11 (e.g., Fig. 6a), much as do fibers from coiled tendrils. However, the antibodies to RG-I side chains, such as LM5 and LM6, react only with the primary wall/middle lamellae complex, no internal layer containing these components is present (Fig. 6b). Thus, even though the straight tendrils produce fibers they do not produce gelatinous fibers even after 2 months of emergence.

Discussion

Fiber cells in redvine have a unique cell wall composition and organization and are similar to gelatinous fibers

In this and in a complementary study (C.G. Meloche and K.C. Vaughn, submitted), we have shown that the coiling of redvine tendrils occurs coincidently with the development of a gelatinous-type fiber (Fig. 2). Moreover, these fibers appear to be critical players in allowing the tendrils to coil. The rare tendrils that fail to coil also fail to produce a gelatinous layer (Fig. 6) and fibers in 4-day-old tendrils that are still straight, have yet to develop a gelatinous layer (Fig. 4b). Thus, fibers alone are not sufficient to produce a coiled tendril but only those with a true gelatinous layer.

Although gelatinous fibers have been rarely reported outside woody tissue (White and Robards 1965; Yoshizawa et al. 2000; Tomlinson 2003, although see discussions in Lev-Yadun et al. 2005), the observations described herein strongly support the idea that redvine tendril fibers are indeed gelatinous (or at the very least display the inner layer with a different composition than the S layers similar to gelatinous fibers). First, the redvine tendril fiber cell wall consists of three distinct layers: the primary wall/middle lamella complex and a secondary (S) wall layers consisting of two secondary layers and an inner gelatinous (G) layer. The G layer is enriched in RG-I epitopes (labeling with CCRCM2, LM5 and LM6) and impoverished in lignin (lack of permanganate staining) compared to the secondary wall (S) layers. Thus, in terms of structure, composition and position, fibers in redvine tendrils are similar to G fibers in other tissues (Wardrop and Dadswell 1955; White and Robards 1965; Tomlinson 2003; Donaldson 2001). A distinctive characteristic of G fibers, also observed in redvine tendril fibers, is the artifactual detachment of the G layer when specimens are prepared for microscopy (Clair et al. 2005; C.G. Meloche and K.C. Vaughn, submitted), further strengthening our analyses that the redvine tendril fibers are properly classified as G fibers.

Areas of the primary wall and the middle lamellae appear to have pectin constituents and organization typical of primary cell walls, although other cell wall layers do not. In the redvine tendril fibers, we see a similar exclusion of both HG and RG-I from the bulk of the secondary cell wall. An exception occurs in the G layer, however, which is strongly labeled with three different antibodies that recognize RG-I (Table 3), although even this layer is unlabeled with antibodies recognizing HG. An especially strong labeling of the

LM5 and LM6 epitopes occurs at the cell corners between adjacent fiber cells. An increase of pectins at these sites might facilitate the adhesion between adjacent fiber cells so that the fibers act in a more concerted way in causing the coiling or perhaps cushion the cells from the strain of the coiling. The presence of HGs at these sites would also facilitate the cushioning and adhesion.

A model for fiber control of redvine tendril coiling

Although a complete understanding of how gelatinous fibers actually generate the force to cause the twisting of the redvine is tendril is unknown, some of the similarities between those in redvine tendrils and those in tension wood (tissues where such fibers are believed to be the principal factors in causing tree righting) may provide some clues as to how the coiling force is generated. Studies on G fibers in tension wood emphasize the compositional differences between the gelatinous and S layers as a primary agent in causing the fibers to exert a macroscopic bending of the tissue (Clair et al. 2005; Prodhan et al. 1995; Yammamoto 2004). The high degree of crystallinity of the cellulose and the orientation of the microfibrils parallel to the long axis of the cell are unique aspects of the G layer (Wardrop and Dadswell 1955). These differences in chemical composition and structure allow for a relatively high amount of moisture accumulation and subsequent shrinkage in the G layer and relatively less in the S layers. This would tend to cause a net contraction of the cell, with the outer layers contracting in response to shrinkage or extension of the internal layers, creating high degrees of tension (Yammamoto 2004). The macroscopic manifestation of cell wall layer is a twisting to the tendril. Lignin might have a role beyond simply rigidifying the tissue as well. Boyd (1973) speculated that the heavy lignification of the S layers of the gelatinous fibers might contribute to a form of helical checking, so that although the G layer can exert a force on the S layers, they do not result in the complete twisting of the fiber cell, but rather an incremental net movement of the tissue as a whole. Lignin may have another role in actually causing the difference in water content between the layers as lignin could displace water in the S layers, making the hydration potential of the S layers even more different than the G layer. In the case of the redvine tendrils, the fibers exist as a cylinder of tissue with the lignin distributed preferentially nearest the touched surface. This would ensure a greater ability to twist on the outer surface than the inner, much as required for the net movement of the tendril. Other, more subtle variations in wall composition across the cells in the fiber band in the degree, distribution and timing of lignification (as well as other components such as callose) might allow for more subtle nuances in the degree and positioning of the coiling. These changes might allow for an enhanced flexibility, allowing the tendril tremendous latitude to successfully twine about objects of diverse size and shape. Moreover, it is well known that G fibers increase the tensile strength of wood after drying (Clair et al. 2003; Coutand et al. 2004). Redvine tendrils dry relatively early after their emergence (C.G. Meloche and K.C. Vaughn, submitted), so this is another potential advantage of having G fibers in a structure that dries out rapidly but are required to support a large mass of tissue.

How exactly does the differential composition of the cell wall layers in the gelatinous fibers allow for a twisting motion? One of the most severely spirally twisted cell types in plants occurs in the pseudoelaters of hornworts (Renzaglia and Vaughn 2000). As these cells dry, they form extensive spirals, aiding in spore separation and dispersal. The mature pseudoelater cells have cell walls consisting of outer S_1 and inner S_3 bands enriched in xylan (Carafa et al. 2005) between which is interposed a S_2 lacking xylan and enriched in arabinanogalactans (Kremer et al. 2004). The extreme difference in composition between these cell wall layers allows for a differential potential uptake of moisture and a consequent effect on the cell wall as the pseudoelater cells dry. As one layer dries more rapidly than another, the cell wall is forced to twist to accommodate the strain, resulting in coiling. This differential drying forces the twisting of the pseudoelater much as would a similar composition difference in the layers of the cell walls of the fibers in redvine tendrils. Of course the pseudoelaters are free cells whereas the tendril fibers are compact cylinders surrounded by cortical and parenchyma cells external to the fiber band and pith parenchyma and vascular tissue internal to it. Both of these tissues might mitigate the potential twisting ability of the fiber cells and the fiber cells don't really dry although moisture levels between layers could be quite different. We further speculate that differences in wall composition from layer to layer in fiber cells might be responsible for a number of tension and release phenomena in plants, such as violent seed dispersal in *Impatiens* and *Geranium* species.

How universal is this phenomenon?

Could the changes in the redvine tendril be typical of not only tendril formation in other plants but also to vining, in general? It is likely that the process of vining and more specifically tendril formation arose several

times evolutionarily as the morphology of tendrils and the tissues from which they are modified are of several origins. Redvine tendrils seem to be touch-sensitive on all surfaces whereas other species have specific areas that seem to be specifically associated with the ability to sense touch (Darwin 1875; Jaffe and Galston 1969). In some ways, the coiling of the redvine tendril and its ability to perceive touch stimuli is more akin to what we see in the stems of vines that use twining as their only mode of climbing. In these tissues, the stem is sensitive on all surfaces and no specialized cells are found that sense touch. In accordance, at least one vine, the moonvine (*Ipomoea calantha*) has a stem anatomy that resembles the redvine tendril in the presence of gelatinous-type fibers and a stem that rigidifies after the position of the coiling has been determined (K.C. Vaughn et al., unpublished observations). Similarly, Scher et al. (2001) observed an unidentified type of fiber (subsequently determined by us as gelatinous and with a similar composition to the fibers described herein, K.C. Vaughn and C.G. Meloche, unpublished) that increased with the vining of morningglory (*Ipomoea* spp.) stems. Presently, we are extending this study to a wide variety of species having either coiled stems or tendrils to determine if this is a universal or restricted phenomenon. Thus, what we are discovering in the redvine might be at least one of the mechanisms for achieving a twining stem as well as a coiled tendril.

Acknowledgments Thanks are extended to Brian Maxwell for technical assistance on both the growing of the redvine plants and the light microscopic photography in this paper. Extremely helpful discussions with Rick Turley, Tobias Baskin and Roberto Ligrone and comments from three anonymous reviewers are acknowledged here. Generous gifts of antibodies from Andrew Staehelin and Michael Hahn are acknowledged that have greatly enhanced this study. Christopher G. Meloche is supported by the in-house ARS Research Associate program. Mention of a trademark, proprietary product or vendor does not constitute an endorsement by USDA.

References

Anderson MA, Sandrin MS, Clake AE (1984) A high proportion of hybridomas raised to a plant extract secrete antibodies to arabinose or galactose. Plant Physiol 75:1013–1016

Boyd JD (1973) Helical fissures in compression wood: causative factors and mechanics of development. Wood Sci Technol 7:92–111

Carafa A, Duckett JG, Knox JP, Ligrone R (2005) Xylan distribution and basal relationships in land plants. New Phytol 168:231–240

Clair B, Ruelle J, Thibaut B (2003) Relationship between stresses, mechano-physical properties and proportion of fibers with gelatinous layer in chestnut (*Castanea sativa* Mill.). Holzforschung 57:189–195

Clair B, Thibaut B, Sugiyama J (2005) On the detachment of gelatinous layer in tension wood fibre. J Wood Sci 51:213–221

Clausen MH, Willats WGT, Knox JP (2003) Synthetic methyl hexagalacturonate hapten inhibitors of anti-homogalacturonan monoclonal antibodies LM7, JIM5 and JIM7. Carbohydr Res 338:1797–1800

Coutand C, Jernimidis G, Chanson B, Loup C (2004) Comparison of mechanical properties of tension and opposite wood in *Populus*. Wood Sci Technol 38:11–24

Darwin C (1875) The movements and habits of climbing plants. Henry Murray, London

Donaldson LA (2001) Lignin and lignin topochemistry—an ultrastructural view. Phytochemistry 57:859–873

Esau K (1977) Anatomy of seed plants. Wiley, New York

Fisher JB, Tomlinson B (2002) Tension wood fibers are related to gravitropic movement of red mangrove (*Rhizophora mangle*) seedlings. J Plant Res 115:39–45

Freshour G, Clay RP, Fuller MS, Albersheim P, Darvill AG, Hahn MG (1996) Development and tissue-specific structural alterations of cell wall polysaccharides of the *Arabidopsis thaliana* root. Plant Physiol 110:1413–1429

Goujon T, Ferret V, Mila I, Polet B, Ruel K, Burlat V, Joseleau JP, Barriere Y, Lapierre C, Jouanin L (2003) Down-regulation of the ArCCR1 gene in *Arabidopsis thaliana* effects on phenotype, lignin and cell wall degradability. Planta 217:218–228

He XQ, Suzuki K, Kitamura S, Lin JX, Cui KM, Itoh T (2002) Toward understanding the different functions of two types of parenchyma cells in bamboo culms. Plant Cell Physiol 43:186–195

Hepler PK, Fosket DE, Newcomb EH (1970) Lignification during secondary wall formation in *Coleus*: an electron microscopic study. Am J Bot 57:85–96

Jaffe MJ (1980) On the mechanism of contact coiling of tendrils. In: Skoog F (ed) Plant growth substances 1979. Springer, Berlin Heidelberg New York, pp. 481–495

Jaffe MJ, Galston AW (1969) The physiology of tendrils. Annu Rev Plant Physiology 417–434

Jones L, Seymour GB, Knox JP (1997) Localization of pectic galactan in tomato pericarp cell walls using a monoclonal antibody specific to (1→4) b-D-galactan. Plant Physiol 113:1405–1412

Kremer C, Pettolino F, Bacic A, Drinnan A (2004) Distribution of cell wall components in *Sphagnum* hyaline cells and in liverwort and hornwort elaters. Planta 219:1023–1035

Lev-Yadun S, Wyatt SE, Flaisman ME (2005) The inflorescence stem fibers of *Arabidopsis thaliana Revoluta (ifl1)* mutant. J Plant Growth Regul 23:301–306

Ligrone R, Vaughn KC, Renzaglia KS, Knox JP, Duckett JG (2002) Diversity in the distribution of polysaccharide and glycoprotein epitopes in the cell walls of bryophytes: new evidence for the multiple evolution of water conducting cells. New Phytol 156:491–508

McCartney L, Gilbert HJ, Bolam DN, Boraston AB, Knox JP (2004) Glycoside hydrolase carbohydrate-binding modules as molecular probes for the analysis of plant cell wall polymers. Anal Biochem 326:49–54

McCartney L, Marcus SE, Knox JP (2005) Monoclonal antibodies to plant cell wall xylans and arabinoxylans. J Histochem Cytochem 53:543–546

Meikle J, Boning I, Hoogenraad N, Carke AE, Stone BA (1991) The localization of (1→3) B-glucans in the cell walls of pollen tubes using specific (1→) B-glucan specific monoclonal antibodies. Planta 185:1–8

Moore PJ, Darvill AG, Albersheim P, Staehelin LA (1986) Immunogold localization of xyloglucan and rhamnogalacturonan 1 in the cell walls of suspension cultured sycamore cells. Plant Physiol 82:787–794

Northcote DH, Davey R, Lay J (1989) Use of antisera to localize callose, xylan and arabinogalactan in the cell plate, primary and secondary walls of plant cells. Planta 178:353–366

Prodhan AKMA, Funada R, Ohtani J, Abe H, Fukuzawa K (1995) Orientation of microfibrils and microtubules in developing tension wood of Japanese ash (*Fraxinus manshuria* var. *japonica*). Planta 196:577–585

Puhlman J, Bucheli E, Swain MJ, Dunning N, Albersheim P, Hahyn MG (1994) Generation of monoclonal antibodies against plant cell walls. I. Characterization of a monoclonal antibody to a terminal (1→2)-linked fucosyl-containing epitopes. Plant Physiol 104:699–710

Renzaglia KS, Vaughn KC (2000) Anatomy, development and classification of hornworts. In: Shaw AJ, Goffinet B (eds) Bryophyte biology. Cambridge University Press, Cambridge, pp. 1–20

Sabba RP, Durso NA, Vaughn KC (1999) Structural and immunocytochemical characterization of dichlobenil-habituated tobacco BY-2 cells. Int J Plant Sci 160:275–290

Scher JL, Holbrook NM, Silk WK (2001) Temporal and spatial patterns of twining force and lignification in stems of *Ipomoea pupurea*. Planta 213:192–198

Smallwood M, Beven A, Donovan N, Neilll SJ, Pearl J, Roberts K, Knox JP (1994) Localization of cell wall proteins in relation to the developmental anatomy of the carrot root apex. Plant J 5:237–245

Smallwood M, Martin H, Knox JP (1995) An epitope of rice threonine- and hydroxyproline-rich glycoprotein is common to cell wall and hydrophobic plasma-membrane glycoproteins. Planta 196:510–522

Tomlinson PB (2003) Development of gelatinous (reaction) fibers in stems of *Gnetum gnemon* (Gnetales). Am J Bot 90:965–972

Vaughn KC (2003) Dodder hyphae invade the host: a structural and immunocytochemical characterization. Protoplasma 220:189–200

Vaughn KC (2006) The abnormal cell plates formed after microtubule disrupter herbicide treatment are enriched in callose. Pestic Biochem Physiol 84:63–71

Vaughn KC, Hoffman JC, Hahn MG, Staehelin LA (1996) The herbicide dichlobenil disrupts cell plate formation: immunogold characterization. Protoplasma 194:117–132

Wardrop AB, Dadswell HE (1955) The nature of reaction wood. IV. Variations in cell wall organization of tension wood fibres. Aust J Bot 3:177–187

White DJB, Robards AW (1965) Gelatinous fibers in ash (*Fraxinus excelsior* L.). Nature 205:818

Willats WGT, Marcus SE, Knox JP (1998) Generation of a monoclonal antibody specific to (1→5) a-L-arabinan. Carbohydrate Res 308:149–152

Yammamoto HY (2004) Role of the gelatinous layer on the origin of the physical properties of the tension wood. J Wood Sci 50:197–208

Yoshizawa N, Inami A, Miyake S, Ishiguri F, Yokota S (2000) Anatomy and lignin distribution of reaction wood in two *Magnolia* species. Wood Sci Technol 34:183–196

Zhong R, Burk DH, Ye ZH (2001) Fibers. A model system for studying cell differentiation, cell elongation and cell wall biosynthesis. Plant Physiol 126:477–479